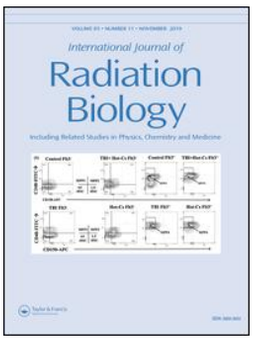

International Journal of Radiation Biology

ISSN: (Print) (Online) Journal homepage: https://www.tandfonline.com/loi/irab20

The New Zealand white rabbit animal model of acute radiation syndrome: hematopoietic and coagulation-based parameters by radiation dose following supportive care

Andre Paredes , Matthew Lindeblad , Rachana Patil , Matthew D. Neal , Yuanfan Hong , Brett Smith , Joy P. Nanda , Vasileios Mousafeiris , John Moulder , Maarten C. Bosland , Alexander Lyubimov & Amelia Bartholomew

To cite this article: Andre Paredes , Matthew Lindeblad , Rachana Patil , Matthew D. Neal , Yuanfan Hong , Brett Smith , Joy P. Nanda , Vasileios Mousafeiris , John Moulder , Maarten C. Bosland , Alexander Lyubimov & Amelia Bartholomew (2020): The New Zealand white rabbit animal model of acute radiation syndrome: hematopoietic and coagulation-based parameters by radiation dose following supportive care, International Journal of Radiation Biology, DOI: 10.1080/09553002.2020.1820606

To link to this article: https://doi.org/10.1080/09553002.2020.1820606

INTERNATIONAL JOURNAL OF RADIATION BIOLOGY
https://doi.org/10.1080/09553002.2020.1820606

Taylor & Francis
Taylor & Francis Group

ORIGINAL ARTICLE

The New Zealand white rabbit animal model of acute radiation syndrome: hematopoietic and coagulation-based parameters by radiation dose following supportive care

Andre Paredes[a], Matthew Lindeblad[b], Rachana Patil[a], Matthew D. Neal[c], Yuanfan Hong[a], Brett Smith[d], Joy P. Nanda[e], Vasileios Mousafeiris[a], John Moulder[f], Maarten C. Bosland[g], Alexander Lyubimov[b], and Amelia Bartholomew[a]

[a]Department of Surgery, University of Illinois at Chicago, Chicago, IL, USA; [b]Department of Pharmacology, University of Illinois at Chicago, Chicago, IL, USA; [c]Department of Surgery, University of Pittsburgh, Pittsburgh, PA, USA; [d]Department of Radiation Oncology, University of Illinois at Chicago, Chicago, IL, USA; [e]Community Research Advisory Council for Clinical and Translational Research, Johns Hopkins University, Baltimore, MD, USA; [f]Medical College of Wisconsin, Milwaukee, WI, USA; [g]Department of Pathology, University of Illinois at Chicago, Chicago, IL, USA

ABSTRACT

Purpose: Animal models that accurately reflect human responses to radiation injury are needed for advanced mechanistic investigation and development of effective therapeutics. The rabbit is an established animal model accepted by the FDA for studies of cardiovascular disease, lipid metabolism, the development of anticoagulants, testing of bone implants, and the development of treatments for infectious diseases such as HIV. The purpose of this study was to investigate the New Zealand White (NZW) Rabbit model as a model of acute radiation exposure because of its established similarity to human vascular, immune, and coagulation responses.

Materials and methods: Two sequential studies were performed in a total of 81 male NZW rabbits, 16–20 weeks of age. All animals underwent clinical observations and peripheral blood analyses following a single dose of 0, 6, 7, 8, 8.5, 9, or 10 Gy of total body irradiation via a 6 MV Linear accelerator photon source on day 0. Animals were treated with timed release fentanyl patch (days 0–30), subcutaneous hydration (day 1, Study 2 only), and oral sulfamethoxazole/trimethoprim 30 mg/kg once daily (days 3–30) and were followed for 30 days or to time of mortality.

Results: Study 1 revealed the estimated LD30, −50, −70, and −90 with 95% confidence intervals (CI) at 30 days to be 6.7 (CI: 5.9–7.4), 7.3 (CI: 6.7–7.8), 7.9 (CI: 7.3–8.4), and 8.8 (CI: 7.9–9.7) Gy, respectively. In study 2, a survey of blood coagulation and biochemical parameters were performed over time and necropsy. Complete blood counts taken from animals exposed to 7, 8, or 10 Gy, demonstrated dose-dependent depletion of lymphocytes, neutrophils, and platelets. Platelet counts recovered to baseline levels in survivors by day 30, whereas lymphocyte and neutrophil counts did not. Decedent animals demonstrated grade 3 or 4 neutropenia and lymphopenia at time of death; 64% of the decedents experienced a 30% or greater drop in hematocrit. Decedent animals demonstrated more than 100% increases from serum baseline levels of blood urea nitrogen, creatinine, aspartate aminotransferase, and triglyceride levels at the time of death whereas survivors on average demonstrated modest or no elevation.

Conclusion: This NZW rabbit model demonstrates dose-dependent depletion of hematopoietic parameters. The $LD_{50/30}$ of 7.8 Gy (95% CI: 6.6–8.4) with supportive care appears to be close to the ranges reported for rhesus macaques (5.25–7.44 Gy) and humans (6–8 Gy) with supportive care. These findings support the utility of the NZW rabbit model for further mechanistic investigation of acute radiation exposure and medical countermeasure testing.

ARTICLE HISTORY
Received 5 November 2019
Revised 5 March 2020
Accepted 1 April 2020

KEYWORDS
Rabbit; total body irradiation; radiation injury; hematopoietic response; acute radiation syndrome; dose response

Introduction

In the event of a nuclear detonation or accident, large populations will be at risk for radiation exposure. Acute radiation exposure can result in cell injury, organ dysfunction, and death. Without supportive medical care, it has been estimated that 50% of persons receiving a radiation dose of 3.5 Gy will die within 60 days (IAEA 1998; AFRRI, and Armed Forces Radiobiology Research Institute 2003). Supportive care regimens can improve the prognosis of radiation-exposure victims and have included different

CONTACT Andre Paredes adpared@gmail.com Department of Surgery, University of Illinois at Chicago, 808 South Wolcott, Suite 5060, Chicago, IL 60712, USA

Supplemental data for this article can be accessed here.

combinations of therapies including intravenous hydration, antibiotics, transfusion of blood products, cytokines, and hematopoietic stem cell transplants, (Stenke et al. 2018). The radiation dose resulting in 50% mortality, 30 days following radiation (LD50/30) for individuals exposed to radiation at the 1986 Chernobyl power plant accident could have been increased from 2.5 to 4.5 Gy (Bolus 2001) to the range of 6–8 Gy if patients received supportive care (Mettler et al. 2007). However, resource intensive supportive care may provide logistical challenges when deployed at the scale needed for large populations after a nuclear or radiological event (Dainiak 2018; Stenke et al. 2018). A better understanding of the mechanisms involved is needed to develop new radiomitigators that can be deployed for large populations (Anno et al. 1989).

Natural history studies of animal models facilitate mechanistic insights of radiation injury and in turn, the development of new radiomitigators (FDA 2009; Williams et al. 2010; Singh et al. 2015). Non-human primate (NHP) models have been regarded as a gold standard for their significant genetic and physiologic similarity to humans(Singh and Olabisi 2017); with supportive care, NHP's have a similar LD50/30 as humans (5.25–7.44) (Eldred and Trowbridge 1954; Henschke and Morton 1957; Broerse et al. 1978; Zoetelief et al. 1998; Yu et al. 2015). NHP radiation studies are typically reserved for advanced testing due to the expertise required in husbandry and care, the stringent ethical justifications, and the need for a variety of highly specialized trained personnel such as primatologists, radiobiologists, ethicists, infectious disease specialists, and others. Other large animal models, such as canines and minipigs, demonstrate advantages over small rodent models due to greater tissue mass and depth dosage, allowing for longitudinal, serial peripheral blood sampling over extended periods of time. In addition, post-radiation hematopoietic kinetics, as well as radiation-induced organ damage, are similar to humans (Carsten 1984), though canines and Gottingen minipigs appear to be more radiosensitive than humans and NHPs (Broerse and Macvittie 2012). Estimations of the LD50/30 in canines range from 2.6 to 3.9 Gy (Norris et al. 1968; MacVittie et al. 2005) and in minipigs from 1.7 to 3.7 Gy, with estimates differing according to source of radioactivity, dose rate, supportive care regimen, and strain (Tullis et al. 1949; Rust et al. 1954; Jones et al. 1986; Morris and Jones 1989; Moroni et al. 2011).

The rabbit model is accepted by the FDA for studies in cardiovascular disease and lipid metabolism (Fan et al. 2015), the development of anticoagulants (Gitel and Wessler 1983), testing of bone and dental implants (Mapara et al. 2012), and the development of treatments for infectious diseases such as HIV (Peng et al. 2015). The established depth and granularity of the rabbit model in cardiovascular and coagulation investigation is particularly attractive for radiation studies given the finding that radiation immediately causes endothelium disequilibrium and injury (Shirota and Tavassoli 1992; Paris et al. 2001; Takatsuka et al. 2002) and survivors of radiation suffer from accelerated cardiovascular disease (Takahashi et al. 2013; Ozasa et al. 2016; Wang et al. 2016; Schollnberger et al. 2018). The rabbit is an established model of acute radiation exposure and has previously been reported to have a LD50/30 in the range of 7–9 Gy (Painter and Brues 1949; Grahn et al. 1956; Andrews 1958). This study's objective was to further define the natural history of hematopoietic, biochemical, and coagulation parameters in response to acute radiation to help identify clinically relevant parameters for future mechanistic investigation and medical counter measure testing.

Materials and methods

Animals

Two studies were performed using a total of 81 New Zealand White male rabbits, which were purchased at 14–18 weeks old, from Charles River Laboratories and were acclimated for at least two weeks before irradiation. Rabbits had a weight range of 2.82–3.38 kg and an age range of 16–20 weeks at time of irradiation. Peripheral blood was collected via venipuncture from the medial ear artery. Temperature was measured using an implantable programmable temperature transponder (IPTT-300, Biomedic Data Systems, Seaford, DE) inserted subcutaneously between the shoulders. Heart rate was measured using a pulse-oximeter or stethoscope. All procedures were performed according to protocols approved by the University of Illinois Animal Care and Use Committee.

Experiment design

Two separate studies, in which animals were irradiated and then followed for 30 days were performed: a dose finding study (study 1) and a follow-up study (study 2). The first (study 1) was a radiation dose–response study performed to define the lethal dose (LD) at 30 days using 49 rabbits that were followed for 30 days post-radiation at the following doses: 0 Gy ($n = 2$, naïve), 6 Gy ($n = 6$), 7 Gy ($n = 10$), 8 Gy ($n = 10$), 8.5 Gy ($n = 10$), 9 Gy ($n = 5$), and 10 Gy ($n = 6$). A sample size of two naïve animals was primarily used for normal tissue controls in pathology and blood analyses over time. The other sample sizes were selected to ensure a projected $n = 6$ of survived animals by end of study at 30 days based on expected radiation-induced mortality rates. Because this was a new study to identify the ranges of radiation responses (study 1) and biomarker kinetics (study 2) the studies were performed in male animals with the expectation that subsequent follow-on studies would be performed with greater granularity, focusing on high yield biomarkers in both sexes. This report provides information on our initial investigations.

The following hematopoietic and coagulation blood parameters were measured pre-radiation twice and at post-radiation days 1, 17, and 30 or at moribund euthanasia when feasible (days 17 and 30 hematopoietic and coagulations measures are not included). The time points were selected to identify rapidly changing biomarkers in response to radiation (day 1), to determine how biomarkers changed

during hematopoietic reconstitution (day 17), and to identify the sustainability of any changes observed (day 30) when compared to pre-radiation levels.

Complete blood counts (*CBC*): Peripheral blood was collected in K2EDTA BD microtainers (BD Cat. No. 365974, Tiger Medical, Irvington, NJ) to measure white blood cells (WBC), red blood cells (RBC), hematocrit (HCT), mean corpuscular volume (MCV), reticulocytes (RET), platelets (PLT), and mean platelet volume (MPV). Differentials were performed and reported as a percentage of the WBC. Data was acquired via an Advia 2120 Analyzer (Siemens, Malvern, PA)and data output was directly downloaded into the Provantis System (Instem, Staffordshire, UK).

For the purposes of this report, we used published reports on normative ranges for New Zealand rabbits(Hewitt et al. 1989; Suckow et al. 2012) as well as our own pretest data. Since the severity of cytopenias post-radiation have not yet been defined in the rabbit model, human definitions of degrees 3 and 4 severities (Waselenko et al. 2004) which track with mortality, were used to examine mortality in the rabbit model. For degree 3 lymphopenia, the human definition, 1.00×10^3 cells/μL, was higher than the lower limits of normative rabbit ranges, 0.75×10^3 cells/μL; this lower limit of normative range served as the upper limit of the definition of degree 3 lymphopenia. We observed that the lymphopenic categories could be extended to an ultralow category, termed 4B in which lymphocyte counts were $<0.1 \times 10^3$ cells/μL. For blood loss, in lieu of hemoglobin as originally described by Daniak (Waselenko et al. 2004), we used hematocrit. Therefore, Neutropenia was defined as, $<1.04 \times 10^3$ cells/μL with degree 3 as 100–500 cells/μL and degree 4 as <100 cells/μL. Lymphopenia was defined as $<0.75 \times 10^3$ cells/μL with degree 3 as $0.5–0.75 \times 10^3$ cells/μL, degree 4 A, $0.1–0.5 \times 10^3$ cells/μL and degree 4B, $<0.1 \times 10^3$ cells/μL. Thrombocytopenia was defined as, $<112 \times 10^3$ cells/μL, with degree 3, $20–50 \times 10^3$ cells/μLand degree 4, $<20 \times 10^3$ cells/μL. Blood Loss was defined as degree 3, if there was a 10–20% decrease in hematocrit level and degree 4, if there was >20% decrease in hematocrit level.

Neutropenia was defined as, $<1.04 \times 10^3$ cells/μL with degree 3 as 100–500 cells/μL and degree 4 as <100 cells/μL. Lymphopenia was defined as $<0.75 \times 10^3$ cells/μL with degree 3 as $0.5–0.75 \times 10^3$ cells/μL, degree 4 A, $0.1–0.5 \times 10^3$ cells/μL and degree 4B, $<0.1 \times 10^3$ cells/μL. Thrombocytopenia was defined as, $<112 \times 10^3$ cells/μL, with degree 3, $20–50 \times 10^3$ cells/μL and degree 4, $<20 \times 10^3$ cells/μL. Blood loss was defined as degree 3, if there was a 10–20% decrease in hematocrit level and degree 4, if there was > 20% decrease in hematocrit level.

Prothrombin time (PT), activated partial thromboplastin time (PTT), fibrinogen, D-dimer, anti-thrombin III: Peripheral blood was collected in citrate (BD Vac. Citrate Blue Blood Coll Tube, 2.7 ml, BD Cat. no. 363083) and analyzed in real time via an ACL 7000 (Beckman Coulter Diagnostics, Chaska, MN).

Thrombin-anti-thrombin (TAT) and plasmin-anti-plasmin (PAP): Peripheral blood was collected in K2EDTA microtainers, plasma separated and cryopreserved in aliquots for batch processing using the ELISA rabbit-specific kit, MyBioSource, Cat. no. MBS703595, San Diego, CA (for TAT) and MyBioSource, Cat. no. MBS703595 (for PAP), according to manufacturer's instructions.

Protein C and activated protein C (APC): Peripheral blood was collected in K2EDTA BD microtainers and plasma was separated and cryopreserved in aliquots for batch processing. Protein C was quantified using ELISA kit, Rabbit Protein C ELISA Kit from MyBioSoure, Cat. no. MBS723552. Activated Protein C was measured using ELISA, MyBioSource, Cat. .o. MBS021088. Both were performed according to manufacturer's instructions.

Coagulation factors II, V, VII, VIII, IX, X, XI, and XII: Peripheral blood was collected in citrate from a subset of animals; plasma was separated and cryopreserved in aliquots for batch processing using the STAGO STart 4 Hemostasis Analyzer and associated reagents (all from Diagnostica Stago, Inc., Parsippany, NJ). Plasma (200 μL) was diluted in 1800 μL of buffer for a 1:10 dilution prior to analyzing the samples according to manufacturer's instructions. Assays were performed according to manufacturers' instructions. STA-Unicalibrator, Cat. no. 00675, and STA-System Control N + P, Cat. No. 00678, were run at the beginning of each analysis for each day of analysis. Samples were kept on ice while being analyzed for factors. Due to activity loss with room temperature storage, care was taken to only thaw samples that could be analyzed within 2 h of thaw.

Thrombin generation assay (*TGA*): Peripheral blood was collected from a subset of animals in the same citrate tube as for PT to conserve the amount of blood drawn and placed into anticoagulant; plasma was separated and cryopreserved in aliquots for batch processing undiluted using fluorometric assay supplied by Technothrombin Thrombin Generation Assay (TGA), Cat. no. 5006010, Teconoclone, DiaPharma (West Chester, OH), according to manufacturer's directions. The kinetics of thrombin generation over 60 min was measured by a BioTeck plate reader (BioTek, Winooski, VT). The following reagents were tested including arachidonic acid (ASCI), ASPI (lyophilized Arachidonic Acid, 0.5 mM), ADP (lyophilized preparation of adenosine-5′-diphosphate, stock concentration 0.2 mM), and Collagen (lyophilized preparation of Type I collagen, stock activity equivalent to 100 μg/mL), all purchased from DiaPharma, were used as agonists. Collagen and ASPI demonstrated greater variability than ADP, which provoked a more heightened and consistent response than the other agonists and was selected as the main agonist for aggregometry reported .

Thromboelastography: Peripheral blood was collected in citrate as described above and analyzed in real time via the TEG 5000 Thromboelastograph Hemostasis Analyzer System, Haemonetics (Boston, MA). TEG500 assay sampling was performed manually using recalcification with 20 μL of calcium carbonate solution (Cat. no. 7003) and activation by kaolin (Cat. no. 6300). Level I (Cat. no. 8001) normal control and Level II abnormal control (Cat. no. 8002) were performed daily as part of routine instrument quality assurance.

Serum electrolytes total calcium, chloride, glucose, potassium, sodium, kidney function tests BUN and Creatinine, and liver function tests alanine aminotransferase (ALT), albumin, alkaline phosphatase, Aspartate Aminotransferase (AST), total bilirubin, total protein: Peripheral blood was collected without additives, (BD Microtainer Red Tube no additive, Cat. no. 365963) and serum was separated and analyzed in real time via Beckman Coulter Model #AU400 Chemistry Analyzer (Beckman Coulter, Franklin Lakes, NJ).

In the second study (study 2), 32 animals were randomized to one of four radiation dose groups (0 Gy ($n = 4$), 7 Gy ($n = 9$), 8 Gy ($n = 14$), and 10 Gy ($n = 5$)) and were given a single dose of intravenous fluids, 100 mL normal saline on day 1 after the blood draws performed for the first 24 h period. The sample size was based on achieving 5–6 evaluable subjects at day 30, taking into account projected mortality. In the case of 10 Gy, the biomarkers evaluated appeared to change substantively in the first week and a sample size was selected to demonstrate these changes. Peripheral blood sampling was collected to define the kinetics of hemostatic and coagulation parameters that demonstrated day 1 changes of animals in study 1 (Table 1).

Irradiation procedure and dosimetry

Animals were sedated with ketamine (30 mg/kg, SC) and xylazine (3 mg/kg, SC), placed in pairs into a custom designed restraint box on their sides, and placed into the 6 MV LINAC photon source (Varian model TrueBeam). Fifty percent of the radiation dose was delivered to one side of the animal followed by rotation of the gantry to complete the remaining 50% of the dose to the opposite side. Radiation was delivered to the specified uniform, total body, midline tissue dose at a dose rate of approximately 86 cGy/min. Verification of the dose delivery was achieved by using a PTW 31010 0.1 cc Semiflex Ion chamber placed within a cylindrical solid Lucite phantom within a predetermined position within the radiation field. Radiation dosimetry demonstrating dose measurements to within −0.2 to 2.0% of the targeted dose.

Post-radiation care

All animals received supportive care consisting of daily analgesia (fentanyl time-release patch; 25 μg/h) from post-radiation days 0–30, and Bactrim (sulfamethoxazole/trimethoprim, 30 mg/kg) once daily from post-radiation days 3–30. In the second study, a single dose of subcutaneous fluids (Lactated Ringer's Solution, 60 mL) was given to all animals on day 1 post-radiation after blood sampling to compensate for the volume of blood collected on day 0 and 1. Animals were observed twice daily for physical signs of pain or distress with more frequent round the clock observations every 1–4 h, during the expected lethality periods of days 10–15. Body temperatures were taken via implanted microchip twice daily in pretest and from post-radiation days 0–30. Body weights were measured before radiation and on post-radiation days 0, 1, 3, 5, 8, 10, 12, 15, 18, 22, 25, and 30. Quantitative measurement of food consumption was performed daily from pre-radiation day −7 until post-radiation day 30.

Table 1. Kaplan–Meier survival table (study 1).

Dose (Gy)	No. of animals	No. of animals dead	30 Day death probability
0	2	0	0
6	6	1	0.167
7	10	4	0.4
8	10	7	0.7
8.5	10	8	0.8
9	5	5	1
10	6	6	1

Euthanasia and necropsy

Moribund sacrifice was performed when animals met one or more of 6 criteria:

1. *Respiratory distress* – this condition was defined as labored breathing consistent with lung pathology (e.g. pneumonia), severe dyspnea, or severe cyanosis.
2. Loss of responsiveness – this condition was defined as minimal or absence of response to stimuli.
3. Severe weakness/inability to obtain feed or water defined as either recumbent or extreme reluctance to stand.
4. Weight loss greater than 20% of initial body weight for 3 consecutive days- in this criterion, either there was loss of 20% of initial, pre-radiation body weight for 3 consecutive days, or for 2 days if there was a sharp decline to or below 25% weight loss on the second day of body weight measurements.
5. Nervous system dysfunction or unremitting pain, which was defined as CNS depression manifested as somnolence, seizures (either focal or generalized tonic-clonic activities), paralysis of one or more extremities, or pain unresponsive to analgesic therapy.
6. Excessive blood loss, defined by severe acute unmitigated ongoing hemorrhage as observed by visible bleeding.

Rabbits meeting pre-established euthanasia criteria were evaluated by the Veterinarian and/or Study Director and then underwent moribund sacrifice by an overdose of Euthanasia III (0.4% pentobarbital sodium, 0.27 mL/kg). All staff performing clinical assessments for monitoring morbidities was trained to identify euthanasia criteria for moribund sacrifice. A gross necropsy was performed on each moribund sacrificed animal and all animals surviving to day 30.

Statistics

A Kaplan–Meier analysis was performed to determine mortality kinetics using Graphpad Prism 8.2 (GraphPad Software, La Jolla, CA). A lethality dose probit curve and 95% confidence interval was made to mortality data using a generalized linear model with logit link function using R-statistical software 3.6.1. Hematopoietic and coagulation

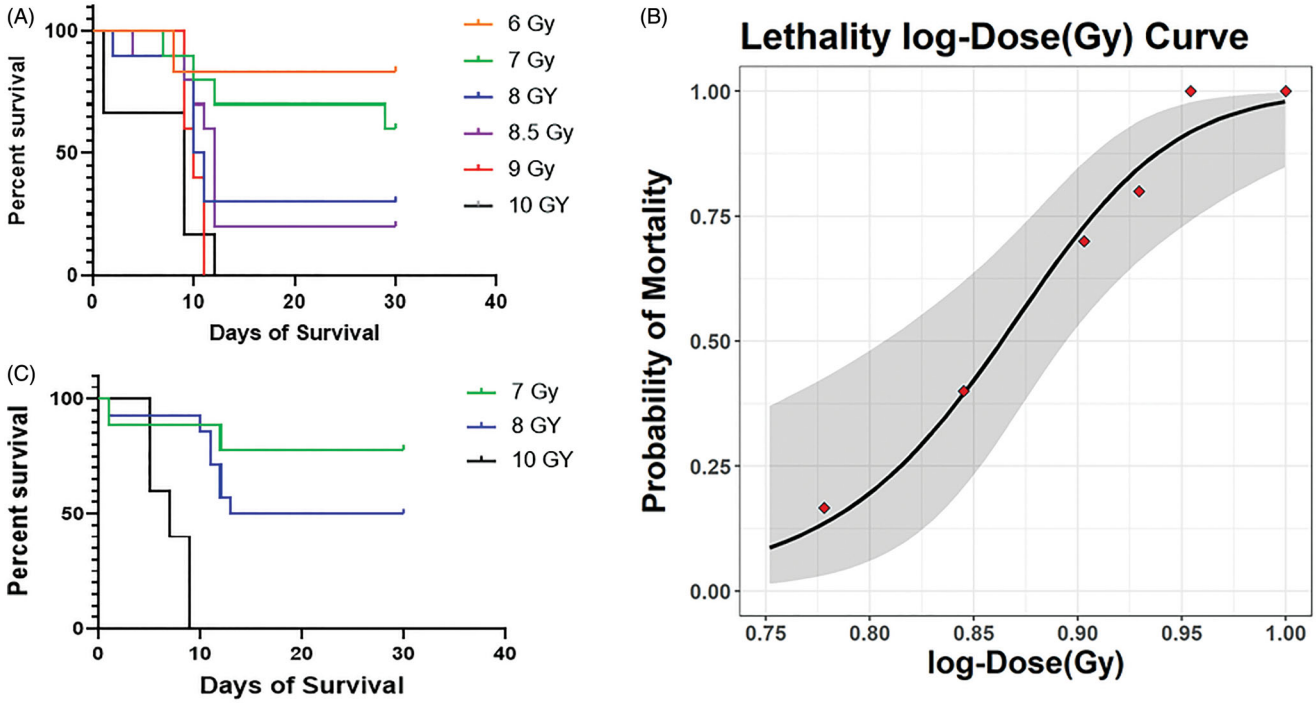

Figure 1. A Kaplan–Meier plot of radiation dose–response, study 1 of 6–10 Gy is shown in (A) and study 2 of 7–10 (Gy) in (C), with the probability of mortality vs log-radiation dose (B, 95% confidence intervals shaded grey).

blood parameters, and additional clinical measures were analyzed for mean and standard deviation; Shapiro–Wilk test was used to test normality. Independent *T*-test or Mann–Whitney test was performed to test for significant differences between radiation groups, survival status, and/or timepoint values. Fisher's exact tests were performed to detect statistically significant categorical associations in clinical signs and body measures between day of survival, radiation groups, and/or time points. To detect large differences between pre-radiation values and post-radiation values, analysis of variance tests were conducted by dose group. If a significant *F* ratio was obtained ($p < 0.05$), Dunnett's *t*-test was used for pair-wise comparisons between each timepoint, including pre-radiation values.

Results

Dose response

In the first study, NZW rabbits were exposed to five radiation doses (6, 7, 8, 8.5, 9, and 10 Gy) and followed for 30 days to determine the lethal dose (LD) at 30 days. The overall 30-day mortalities for these five doses were 16.7%, 40%, 70%, 80%, 100%, and 100%, respectively (Table 1). A mortality curve using this data is presented in Figure 1(A). A probit analyses revealed the estimated LD30, −50, −70, and −90 at 30 days to be 6.7 (95% CI: 5.9–7.4), 7.3 (95% CI: 6.7–7.8), 7.9 (95% CI: 7.3–8.4), and 8.8 (95% CI: 7.9–9.7) Gy (Figure 1(B) and Table 2).

Table 2. Lethality dose probit table (study 1).

30 Day lethal dose (LD)	95% Confidence interval (Gy)	Dose (Gy)
LD30	5.9–7.4	6.7
LD50	6.7–7.8	7.3
LD70	7.3–8.4	7.9
LD90	7.9–9.7	8.8

Clinical signs

Observations of clinical signs were recorded to note possible symptoms related to cause of death for both studies (Supplementary Table 1). Manifestations of neurologic effects included decreased activity, eye closure, and seizure-like activity. Weakness and decreased activity were observed in all dose groups and nearly all animals (survivors and non-survivors, particularly with days 0–7 early deaths), and was observable immediately after irradiation up until day of death. Notably, seizure-like activity was observed in 7 out of 45 non-survivors (deaths on days 1, 5, 9, 11, and 12) as opposed to zero surviving animals, with the trend of association ($p = 0.15$). Signs of bleeding manifested subtly in incidences of bruising in all animals (both survivor and non-survivors). Both surviving and non-surviving animals demonstrated pallor the ears and/or mucous membranes, with the highest frequency observed in the second week post-radiation. Skin changes observed included skin erythema, first observed on day 5 with some animals demonstrating such changes through day 30, and hair loss, first observed on day 7, extending to day 30 in some animals, affecting survivors (days 7–30) and non-survivors (days 7–12) similarly in onset. Notably, when considering gastrointestinal signs, anorexia significantly associated with mortalities (days 1–13) as opposed to survivors, $p < 0.001$. Anorexia was only found in non-survivors above 6 Gy, observable as early as 1-day post-radiation and remaining until day of death. Anorexia was not noted in survivors. Abnormal pulmonary signs observed included labored breathing and nasal congestion with associated discharge; both conditions were

Table 3. Kaplan–Meier survival table (study 2).

Dose (Gy)	No. of animals	No. of animals dead	30 Day death probability
0	4	0	0
7	9	2	0.222
8	14	7	0.5
10	5	5	1

minimally observed non-survivors, occurring as early as 24 h post-radiation. Only 2 out of 45 non-surviving animals were observed with nasal discharge (found only on day 1) as opposed to zero surviving animals.

Early changes in hematological and coagulation parameters

In humans exposed to lethal levels of radiation, depletion of lymphocyte, neutrophil and platelet have been contributed to mortality with rapid changes occurring within the first 24 h (Guskova et al. 1988). Also during this acute time period, radiation-induced endothelial injury results in changes in coagulation responses with increased platelet adherence (Mouthon et al. 2003). Based on these findings, we reasoned that day 1 findings, in study 1, might be an ideal timepoint to identify hematologic and coagulation measures which were likely to be perturbed (Tables 4–7). In study 1, when compared to pre-radiation values, complete blood counts (Table 4), including whole blood cells counts (8, 8.5, and 10 Gy; $p < 0.05$) and reticulocytes (6 and 8.5 Gy; $p < 0.05$) demonstrated significant decreases, while significant increases were noted in hematocrit (8.5 Gy, $p < 0.05$). Most notably, lymphocyte counts (all dose groups, $p < 0.001$), neutrophil counts (all dose groups; $p < 0.001$), and platelet counts (9 Gy; $p = 0.03$) were significantly depressed on day 1 when compared to pre-radiation values, aligning with human hematological disturbances.

Global measures of coagulants at day 1 when compared to pre-radiation values (Table 5) demonstrated significant decreases in platelet aggregates (8.5 Gy, $p < 0.05$), prothrombin time (8.5 and 10 Gy, $p < 0.05$), and significant increases in activated partial thromboplastin time (6, 7, 8, 8.5, and 10 G, $p < 0.05$). Coagulation factors at day 1 when compared to pre-radiation values (Table 6) demonstrated significant decreases in Factor II (7 and 8 Gy, $p < 0.05$), Factor X (9 and 10 Gy, $p < 0.05$), Factor XII (9 Gy, $p < 0.05$), and significant increases in Factor VIII (6, 7, 9, and 10 Gy, $p < 0.05$). Additional day 1 increases were demonstrated in fibrinogen, which functions both in coagulation and as an acute phase reactant (all dose groups; $p < 0.001$) and with TGA (10 Gy; $p < 0.05$) when compared to pre-radiation values.

Anti-coagulants measures at day 1 when compared to pre-radiation values (Table 7) demonstrated significant decreases in anti-thrombin III (7, 8, 9, 10 Gy, $p < 0.05$), d-dimer (8.5, 10 Gy, $p < 0.05$), and plasmin antiplasmin (8.5 Gy, $p < 0.05$). All other study 1 measures demonstrated indeterminable changes across all groups and when compared to pre-radiation values.

Table 4. Pre-radiation and day 1 post-radiation median and range of complete blood counts (study 1).

	Pre-radiation values		Day 1		Day1		Day		Day 1		Day 1		Day 1	
			0 Gy ($n = 2$)		6 Gy ($n = 6$)		7 Gy ($n = 10$		8 Gy ($n = 10$)		8.5 Gy ($n = 10$)		9 Gy ($n = 5$)		10 Gy ($n = 6$)	
Measure (unit)	Median	Range	Median	Range	Median	Range	Median	Range	Median	Range	Median	Range	Median	Range	Median	Range
WBC (10^3/μL)	7.35	(5.32–10.6)	8.41	(7.83–8.98)	4.94	(3.58–8.13)	5.19	(2.02–9.56)	5.52**	(2.18–8.76)	4.60**	(2.71–8.37)	5.27	(2.22–7.96)	4.06**	(3.01–7.9)
ALC (10^3/μL)	5.19	(1.72–7.94)	6.430	(6.03–6.83)	0.500**	(0.27–0.82)	0.490**	(0.14–1)	0.350**	(0.15–1.17)	0.420**	(0.16–0.86)	0.320**	(0.16–0.96)	0.595**	(0.29–1.06)
ANC (10^3/μL)	1.28	(0.475–3.1)	1.35	(1.12–1.57)	4.30**	(2.96–7.34)	4.64**	(1.68–9)	5.06**	(1.8–7.79)	4.30**	(1.74–8.07)	4.70**	(1.19–7.52)	3.40**	(2.4–7.51)
HCT (rel. %)	36.7	(31.7–41.7)	40.4	(39.4–41.5)	38.5	(34.6–41.3)	36.8	(35.4–41.1)	36.4	(34.1–41.3)	39.2**	(36.7–41.4)	34.7	(30.4–36)	34.7	(32–39.7)
RET (10^3/μL)	119	(52.1–247)	152.0	(151–154)	76.6**	(48.6–99.7)	108.0	(64.8–156)	92.9	(48.4–113)	82.8**	(70.1–124)	107.0	(89.3–134)	127.0	(96.7–139)
PLT (10^3/μL)	375	(169–503)	422	(386–457)	312	(260–358)	319	(179–391)	354	(249–399)	352	(229–399)	240**	(207–326)	310	(263–413)

WBC: white blood cells; ALC: absolute lymphocyte count; ANC: absolute neutrophil count; HCT: hematocrit; RET: reticulocytes; PLT: absolute platelet count; (**) indicates significant difference from respective pre-values $p < 0.05$ via analysis of variance followed by Dunnet's procedure.

Table 5. Pre-radiation and day 1 post-radiation median and range of global measures of coagulation (study 1).

			Day 1		Day1		Day		Day 1		Day 1		Day 1	
	Pre-radiation values		0 Gy ($n = 2$)		6 Gy ($n = 6$)		7 Gy ($n = 10$		8 Gy ($n = 10$)		8.5 Gy ($n = 10$)		9 Gy ($n = 5$)		10 Gy ($n = 6$)	
Measure (unit)	Median	Range	Median	Range	Median	Range	Median	Range	Median	Range	Median	Range	Median	Range	Median	Range
AGG (a.u.c.)	50.3	(24.5–205)	40.5	(29–52)	49.0	(21–83)	53.0	(21–75)	52.5	(28.9–59)	63.5	(15–82)	32.0**	(21–50)	52.0	(23–75)
TGA (a.u.c.)	8700	(5230–11100)	7930	(6970–8880)	7480	(6050–14500)	8260	(5610–11300)	9350	(7270–17900)	9040	(7230–13200)	11200	(6560–17000)	11800**	(9540–17400)
PT (sec)	6.3	(6–7.05)	6.52	(6.45–6.6)	6.15	(6–6.15)	6.08	(6–6.15)	6.15	(6–6.45)	6.00**	(6–6.3)	6.15	(6–6.3)	6.00**	(6–6.15)
APTT (sec)	13.4	(7.2–17.4)	14.9	(14.4–15.4)	17.4**	(16.2–22.5)	17.0**	(14.1–21)	17.9**	(12.8–22)	16.6**	(12.9–20.7)	16.0	(8.7–16.8)	19.2**	(17.7–22.6)
TEG–G (d/sc)	11.3	(7.9–14.4)	/	/	20.3	(15–22)	19.6	(17.6–23.9)	14.6	(6.8–19.6)	22.1	(17.8–25.4)	20.6	(9.6–23.1)	17.6	(14.2–26.8)
TEG(degree)	69.9	(13.9–79.6)	/	/	73.7	(67.2–73.8)	76.6	(73.4–78.4)	58.4	(17.1–70.2)	74.8	(71.4–76.5)	71.5	(67.5–78.5)	74.4	(71.9–74.8)
TEG-K (min)	80.8	(48–123)	/	/	75	(66–120)	63	(48–78)	87	(78–126)	72	(60–90)	87	(54–126)	75	(66–84)
TEG-MA(mm)	68.9	(60–74.2)	/	/	80.2	(75.1–81.5)	79.7	(77.8–82.7)	72.7	(57.7–79.7)	81.6	(78.1–83.6)	80.5	(65.7–82.2)	77.6	(74–84.3)
TEG-R(min)	295	(168–474)	/	/	390	(330–600)	270	(204–306)	267	(150–522)	477	(366–570)	345	(222–564)	405	(288–522)

AGG: aggregometry; TGA: thrombin generation assay; APTT: activated partial thromboplastin time; PT: prothrombin time; TEG: thromboelastography; "/" indicates not applicable; TEG was not measured for 0 Gy animals, therefore, no value exists; (**) indicates significant difference from respective pre-values $p < 0.05$ via analysis of variance followed by Dunnet's procedure.

Survival proportions, follow-up study

In study 2, a more discriminant range of doses (7, 8, and 10 Gy) was used to characterize more granularity in the natural history of H-ARS 30 days post irradiation. In this follow-up study, the mortality rates for 0 ($n = 4$), 7 ($n = 9$), 8 ($n = 14$), and 10 ($n = 5$) Gy were 0%, 22%, 50%, and 100%, respectively (Figure 1(C) and Table 3). Most mortalities (64%) occurred between days 9 and 13. For the 7 Gy dose group, we observed one early death on day 1 and one second week death on day 12. For 8 Gy, one death occurred on days 1 and 6 deaths were observed between days 10 and 13. The 10 Gy dose group demonstrated 3 deaths in the first week, and two deaths in the second week up to day 9.

Fever, tachycardia, and weight loss

Early mortality was associated with higher body temperatures and heart rates at time of death. (Figure 2). A dose–response trend was observed day 1, median and range, for 7 Gy (212 bpm, 185–275 bpm), 8 Gy (256 bpm, 120–300 bpm), and 10 Gy (263 bpm, 137–300 bpm, Figure 2(A,B)). However, this did not reach significance and was not noted at other timepoints. Heart rates of non-survivors at moribund sacrifice days (days 1–12) were significantly higher ($p = 0.001$) in median and range (242 bpm, 192–300 bpm) when compared to day 30 schedule sacrificed heart rates (190 bpm, 150–220 bmp).

Body temperatures were recorded via shoulder implanted microchips, with a pre-radiation median value of 101.9 °F (ranging from 101 °F to 103 °F, Figure 2(C,D)). Normative ranges of core body temperatures in NZW rabbits have been documented to be lower than alternative breed counterparts, even in stressed environments (Jimoh and Ewuola 2018). In general, non-survivor and survival animals median body temperatures fell within pre-radiation range of values. However, body temperatures of non-survivors at moribund sacrifice days, ranging from days 1 to 12, were significantly higher ($p = 0.001$) in median and range (104.5 °F, 100.6 °F to 106.6 °F) when compared to day 30 schedule sacrificed body temperatures (101.4 °F, 100.2 °F to 102.8 °F). For both survivors and non-survivors', the day-12 timepoint had the highest percent incidence of body temperatures exceeding 103 °F (50% and 100%, respectively).

Food intake was measured along with body weights to identify potential gastrointestinal effects. Post-radiation overall mean body weight decreased by approximately 2% on day 8 (Figure 2(E,F)). No animal met euthanasia criteria of a 20% or more weight loss.

Red blood cell lineage and response kinetics

The schedule for blood draw in study 2 differed from study 1 by frequency and selectivity of parameters as described in Table 8. Hematocrit levels (Figure 3(A,B)) significantly decreased following exposure when compared to baseline ($p < 0.001$) on days 12, 15, and 17 in the 7 Gy and in the 8 Gy dose group on days 8 and 22, but later recovered in

Table 6. Pre-radiation and day 1 post-radiation median and range of coagulation factors (study 1).

			Day 1		Day1		Day		Day 1		Day 1		Day 1		Day 1	
	Pre-radiation values		0 Gy ($n = 2$)		6 Gy ($n = 6$)		7 Gy ($n = 10$		8 Gy ($n = 10$)		8.5 Gy ($n = 10$)		9 Gy ($n = 5$)		10 Gy ($n = 6$)	
Measure (unit)	Median	Range	Median	Range	Median	Range	Median	Range	Median	Range	Median	Range	Median	Range	Median	Range
FB (g/L)	257	(147–377)	252	(251–253)	759**	(742–848)	687**	(529–764)	645**	(508–729)	743**	(649–878)	664**	(398–768)	729**	(489–804)
F2 (% act.)	100	(87.7–126)	92.6	(88.1–97.1)	96.0	(92.6–110)	92.2**	(87.5–109)	90.4**	(81.6–112)	95.0	(86.6–107)	96.6	(93.2–104)	99.8	(91–105)
F5 (% act.)	93.6	(82.2–182)	85.7	(85.1–86.4)	95.7	(92.8–105)	94.6	(90.7–102)	91.9	(84–97.4)	94.7	(85.7–106)	95.3	(91.4–105)	95.3	(85.3–101)
F7 (% act.)	187	(156–200)	168	(156–180)	179	(146–199)	174	(156–200)	163	(131–200)	179	(130–200)	175	(169–199)	196	(174–200)
F8 (% act.)	179	(116–200)	145	(136–154)	148**	(138–177)	189**	(151–200)	179	(152–200)	162	(146–200)	200**	(188–200)	137**	(114–200)
F9 (% act.)	113	(87.3–165)	101	(97.4–104)	105	(100–149)	123	(87.8–152)	112	(88.9–123)	108	(80.8–159)	132	(121–145)	112	(94.3–135)
F10 (% act.)	120	(105–162)	111	(104–118)	134	(122–158)	131	(116–170)	128	(112–152)	132	(119–161)	137**	(132–156)	150**	(137–169)
F11 (% act.)	128	(91.4–180)	102	(102–103)	123	(102–126)	115	(104–152)	104	(95.4–170)	124	(107–158)	137	(116–166)	113	(107–156)
F12 (% act.)	102	(48–167)	89.2	(83.9–94.4)	102.0	(68.9–139)	95.8	(75.2–144)	97.0	(84.4–152)	122.0	(94–148)	126.0**	(104–167)	112.0	(87–146)

FB: fibrinogen; F2: Factor II; F5: Factor V; F7: Factor VII; F8: Factor VIII; F9: Factor IX; F10: Factor X; F11: Factor XI; F12: Factor XII; (**) indicates significant difference from respective pre-values $p < 0.05$ via analysis of variance followed by Dunnet's procedure.

Table 7. Pre-radiation and day 1 post-radiation median and range of anti-coagulants (study 1).

			Day 1		Day1		Day		Day 1		Day 1		Day 1		Day 1	
	Pre-radiation values		0 Gy ($n = 2$)		6 Gy ($n = 6$)		7 Gy ($n = 10$		8 Gy ($n = 10$)		8.5 Gy ($n = 10$)		9 Gy ($n = 5$)		10 Gy ($n = 6$)	
Measure (unit)	Median	Range	Median	Range	Median	Range	Median	Range	Median	Range	Median	Range	Median	Range	Median	Range
ATIII (%)	127	(94–146)	112.0	(104–119)	117.0	(89–122)	108.0 **	(88–127)	99.0**	(49–111)	120.0	(101–144)	84.0**	(81–119)	98.5**	(74–119)
DD (ng/mL)	193	(164–411)	159	(153–165)	215	(186–227)	180	(114–232)	176	(59.2–239)	172**	(112–211)	190	(25.1–228)	118**	(25.3–190)
APC (ng/mL)	476	(369–655)	457	(436–477)	491	(453–513)	455	(393–536)	449	(410–545)	473	(445–506)	474	(426–528)	434	(389–482)
PAP (ng/mL)	1.1	(0.908–1.63)	0.983	(0.96–1.01)	1.100	(0.95–1.27)	1.150	(0.9–1.38)	0.886	(0.722–1.3)	0.998**	(0.679–1.24)	1.110	(0.934–1.47)	1.130	(0.716–1.48)

ATIII: anti-thrombin III; DD: d-dimer; APC: activated protein C; PAP: plasmin antiplasmin; (**) indicates significant difference from respective pre-values $p < 0.05$ via analysis of variance followed by Dunnet's procedure.

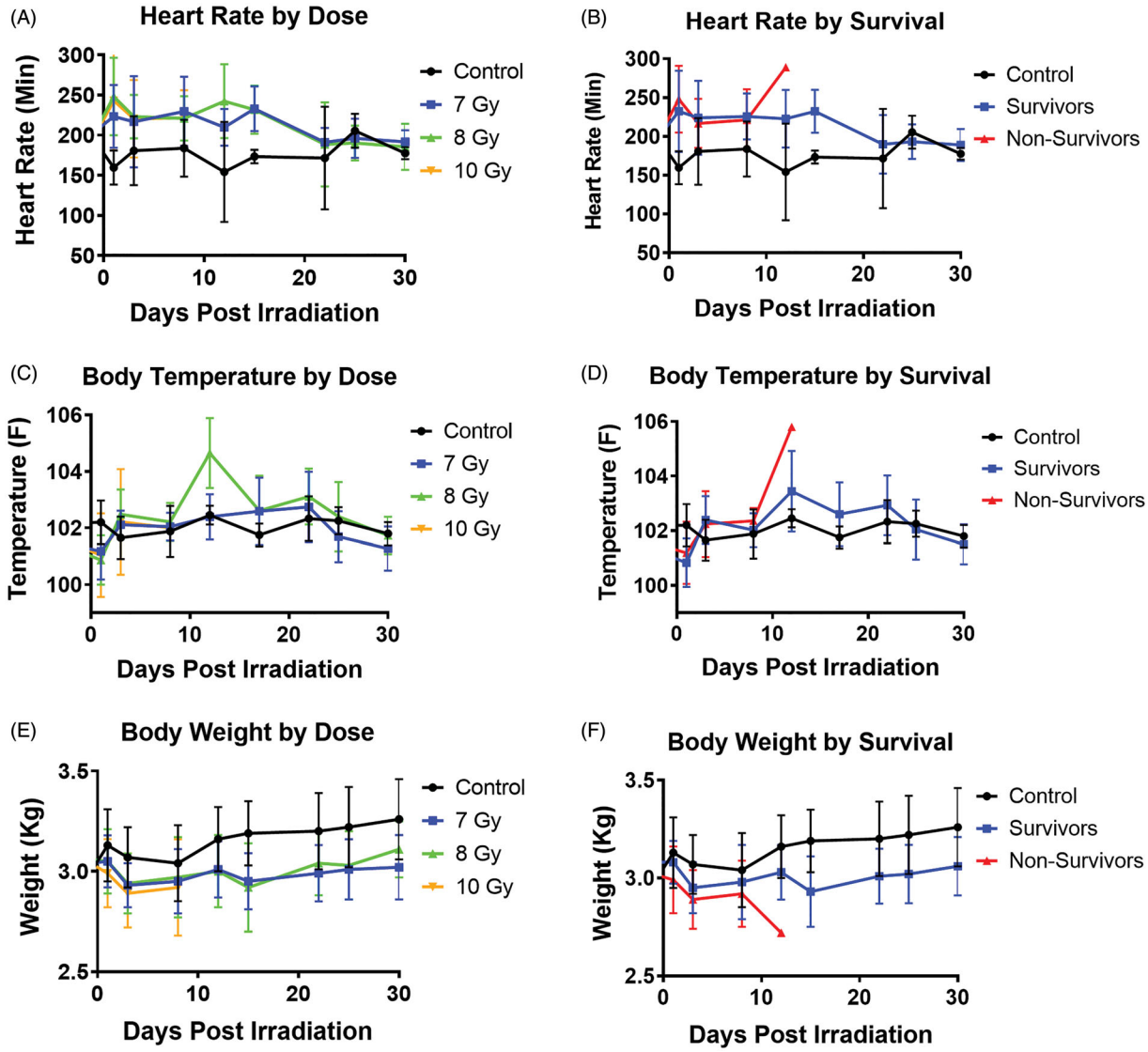

Figure 2. Heart rate (A,B), body temperature (C,D), and body weight (E, F) changes per radiation dose group (A,C,E) and by survival status(B,D,F) with mean ± standard deviation per time point respectively.

Table 8. Schedule of assays performed for study 2.

	CBC	P/AP[a]	APC[b]	Platelet aggregometry	TEG[c]	PT/APTT, fibrinogen, d-dimmer, AT-III, TGA[d]	Blood chem[e]	Tri[f]
Pretest	x	x	x	x	x	x	x	x
1 h	x	x	x		x	x		x
6 h			x	x	x	x		x
Day 1	x	x	x	x	x		x	x
Day 2								x
Day 3	x		x	x	x	x		x
Day 8	x		x		x	x		
Day 12	x		x		x	x	x	x
Day 15	x		x		x			
Day 17	x	x	x	x	x	x		
Day 22	x			x	x			
Day 25	x				x			
Day 30	x	x	x	x	x	x	x	X

[a]Plasmin/anti-plasmin.
[b]Activated protein C.
[c]Thromboelastography.
[d]Thombin generation assay.
[e]Blood chemistries.
[f]Triglycerides.

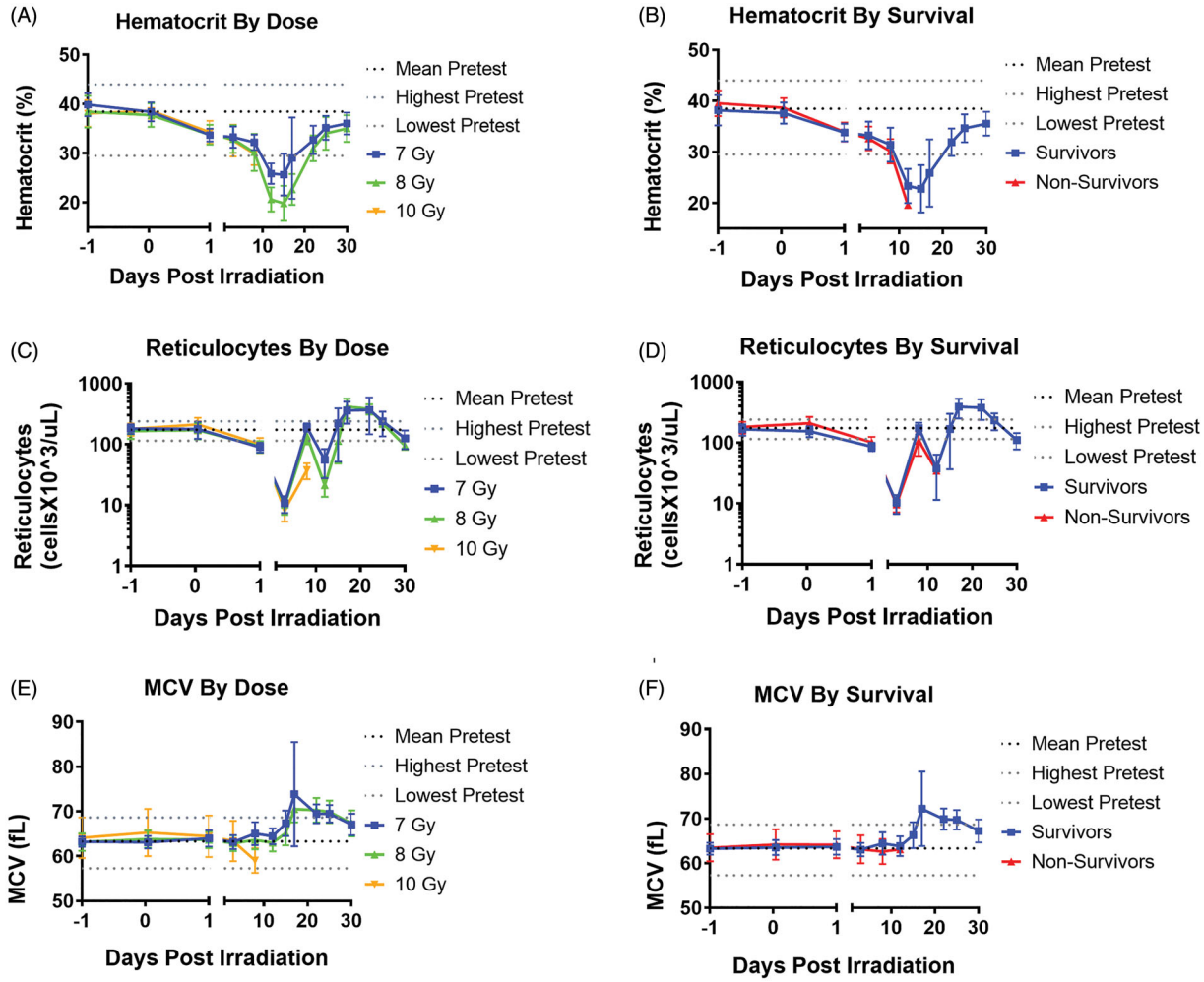

Figure 3. Red blood cell parameters hematocrit (A,B), reticulocytes (C,D) and MCV (E,F) are shown by radiation dose (A,C, E) and by survival status (B, D, F), with mean ± standard deviation per time point respectively. A gap is introduced between days 1 and 2 to represent two separate time scales post- and pre- gap. Horizontal axis days post-irradiation value "−1" indicates a pre-radiation timepoint value and "0" represents the 1-h time point value.

surviving animals. The nadir for the 7 Gy group was 23.8 ± 4.4% and occurred at an average 14.4 ± 2.1 days. The 8 Gy dose group nadir was lower, 20.4 ± 3.5%, and occurred earlier at average 13.4 ± 1.9 days.

Reticulocyte counts (Figure 3(C,D)) of non-survivors were significantly higher ($p = 0.007$) than survivors at 1 h following radiation, with 8 and 10 Gy dose groups exhibiting higher increase compared to 7 Gy. On day 1, reticulocyte levels dropped consistently across all dose groups to nearly half of the baseline. On day 3, further decreases were observed for all three groups to approximately 4–8% of baseline values. By day 8, reticulocyte counts rebounded 100% above baseline for the 7 and 8 Gy dose groups whereas the 10 Gy dose group only increased to a mean of 37.7% of baseline. For the 7 and 8 Gy dose group, reticulocytes continued to increase, reaching approximately 4-fold increases from baseline on days 22 and 17, respectively. At day 30, reticulocyte counts were noted to have decreased to near baseline values. No animal in the 10 Gy group survived past day 12 and their reticulocyte counts were significantly lower ($p < 0.001$) than baseline at time of death. Interestingly, for those animals demonstrating mortality after 8 days in the 7 and 8 Gy dose groups, the reticulocyte counts were ∼50% below baseline. The 10 Gy group, demonstrated a more profound decrease to a mean of 8.4% of baseline values on day 3, suggesting a differential in the magnitude of effect on the bone marrow between the 7 and 8 Gy dose groups compared to the 10 Gy dose group.

Mean corpuscular volume (MCV) (Figure 3(E,F)) observed in survivors of radiation groups 7 and 8 Gy showed slight, non-significant, increases on day 17–14% above baseline values. By days 22 and 25, these increases reached significance in the 7 Gy recipients and in the 8 Gy group, significant increase were noted on day 25 ($p < 0.001$ for both respective groups). In contrast, the 10 Gy group demonstrated decreases from baseline in MCV on day 8 (no statistics were performed in the 10 Gy dose group with $n = 2$ surviving at day 8).

White blood cell lineage and response kinetics

WBC counts (Figure 4(A,B)) significantly decreased in all dose groups ($p < 0.001$) at 1-h post-radiation and 3, 8, 12, 15, 22, 25, and 30 days post-radiation (no statistics were performed in the 10 Gy dose group with $n = 2$ surviving at day 8 and no animals beyond day 12).

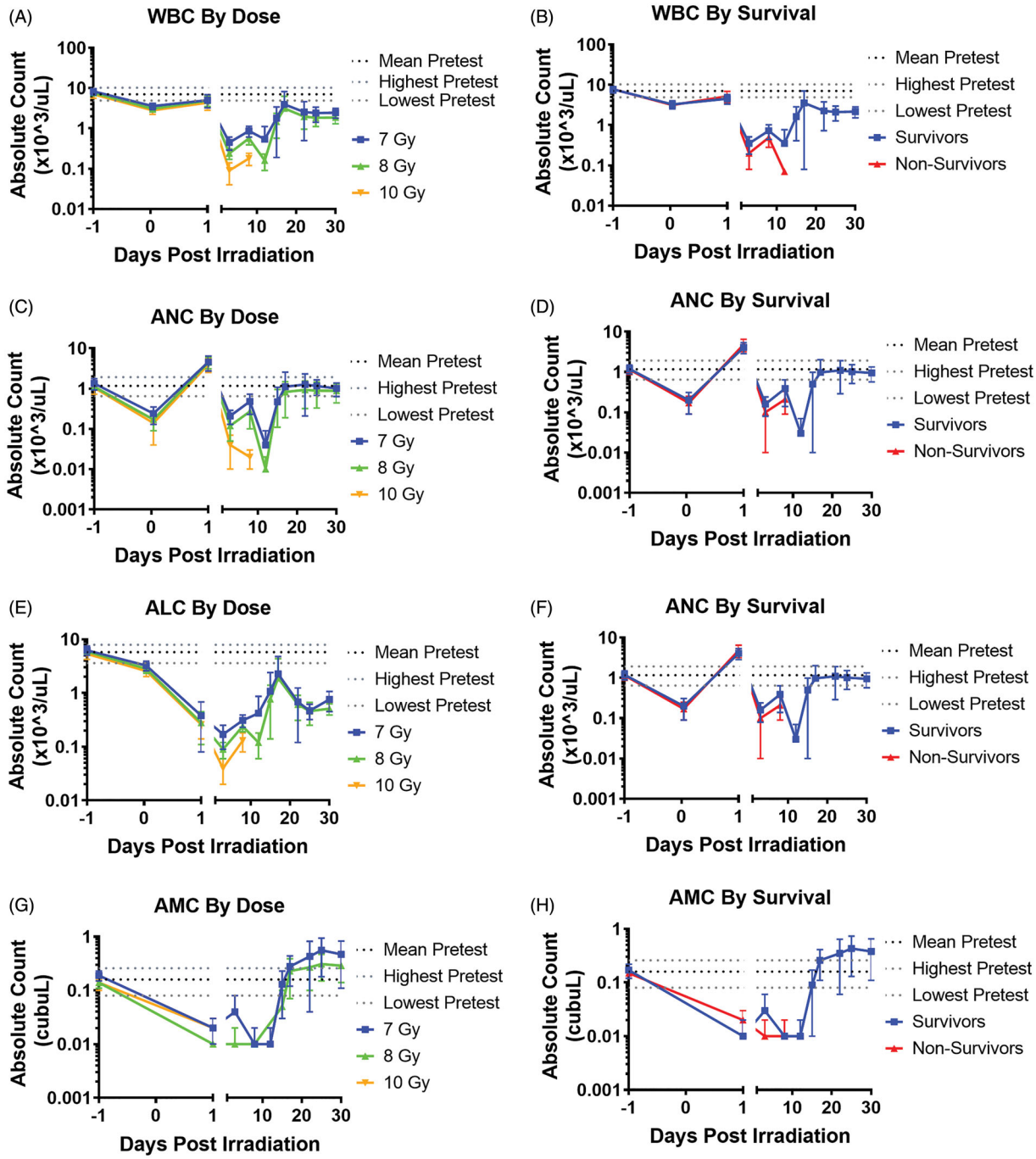

Figure 4. White blood cell parameters including, white blood cell counts, (A,B), absolute neutrophil count, ANC, (C,D), absolute lymphocyte count, ALC, (E,F), and absolute monocyte count, AMC, (G,H) are shown by dose (A,C,E,G) and survivor status (B,D,F,H), with mean ± standard deviation per time point respectively. A gap is introduced between days 1 and 2 to represent two separate time scales post- and pre-gap. Horizontal axis days post-irradiation value "−1" indicates a pre-radiation timepoint value and "0" represents the 1-h time point value.

Absolute neutrophil counts, ANC (Figure 4(C,D)), significantly decreased in all irradiated dose groups at 1-h ($p < 0.001$), then significantly *increased* 3-fold above baseline 24 h after irradiation ($p < 0.01$). ANC showed decreasing values reaching significance on day 12 ($p < 0.001$). The mean ANC nadirs and mean day the nadir was reached for 7,8, and 10 Gy doses were 0.047 ± 0.056 (day 11), 0.017 ± 0.034 (day 10.3), $0.01 \pm 0.005 \times 10^3$ cells/μL (day 5.4), respectively (Table 9). Notably, 42.9% of survivors of 7 Gy sustained recovery of ANC $>10^3$ cells/μL at day 30 while only 28.6% of 8 Gy survivors did. The 8 Gy survivors had a higher frequency of animals which failed to achieve an ANC$> 10^3$ cells/μL in the recovery period when compared to the 7 Gy group, 57.1% versus 28.6%.

Absolute lymphocyte counts, ALC (Figure 4(E, F)), in all radiation groups decreased significantly ($p < 0.001$) at 1-h and demonstrated progressive decreases in timepoints to day 8 when compared to baseline. The mean ALC nadirs and mean day the nadir was reached were 0.18 ± 0.09 (day 3.6), 0.82 ± 0.35 (day 3.9), 0.26 ± 0.16 (day 4.6) $\times$ 10^3 cells/μL for 7, 8, and 10 Gy doses, respectively (Table 9). While some ($n = 6$) survivors, demonstrated transient increases in

Table 9. Hematology nadirs (study 2).

Radiation dose	Nadir (10^3 cells/μL)	Mean day of Nadir	Mean value on day 30	Nadir (10^3 cells/μL)	Mean day of Nadir	Mean value on day 30	Nadir (10^3 cells/μL)	Mean day of Nadir	Mean value on day 30
7 Gy	0.180 ± 0.093	3.6 ± 3.1	0.76 ± 0.31	0.047 ± 0.056	11.0 ± 4.2	1.01 ± 0.37	27.0 ± 36.3	9.0 ± 3.6	305 ± 114
8 Gy	0.082 ± 0.034	3.9 ± 3.2	0.51 ± 0.12	0.017 ± 0.034	10.3 ± 3.7	0.88 ± 0.44	25.4 ± 45.9	9.0 ± 3.2	296 ± 124
10 Gy	0.026 ± 0.016	4.6 ± 2.3	NA	0.010 ± 0.005	5.4 ± 2.5	NA	29.4 ± 42.9	6.0 ± 2.8	NA
Normative range	ALC > 1.5 × 10^3 cells/μL			ANC > 10^3 cells/μL			Platelets >100 × 10^3 cells/μL		

lymphocyte counts post-radiation, none of the 7 or 8 Gy survivors sustained lymphocyte count recovery to an ALC >1500 cells/μL at day 30.

Absolute monocyte counts, AMC (Figure 4(G,H)), overall demonstrated the same pattern as ALC, demonstrating significance ($p < 0.001$) at 1-h, days, 1, 3, 8, and 12 when compared to pre-radiation values. Animals, in all dose groups, that had a monocyte count above 0.03 × 10^3 cells/μL on day 3 significantly ($p < 0.001$) outlived animals that had AMC below that cutoff.

Platelet lineage and response kinetics

Platelet counts (Figure 5(A,B)) significantly decreased at 1-h in all radiation groups from baseline values (versus baseline, 7 Gy recipients, $p < 0.05$; 8 Gy and 10 Gy recipients, < 0.01). However, thrombocytopenia, defined as <100 × 10^3 cells/μL, was not observed until after day 3; severe thrombocytopenia (<20 × 10^3 cells/μL) was observed in all dose groups. The mean PLT nadirs and mean day the nadir was reached were 27 ± 36 (day 9), 25 ± 46 (day 9), and 29 ± 43 (day 6) × 10^3 cells/μL (day 5.4) for 7, 8, and 10 Gy doses, respectively (Table 9). On day 12, depressions in platelet counts continued to be significantly lower than baseline values in dose groups, 7 and 8 Gy ($p < 0.001$). By day 30, both 7 and 8 Gy groups achieved recovery of platelets > 100 × 10^3 cells/μL.

Mean platelet volume, MPV (Figure 5(C,D)), on days 3 and 8 significantly increased relative to baseline values ($p < 0.001$) in all dose groups and in the 8 Gy dose group on days 15 and 25 ($p < 0.01$) and day 30 ($p < 0.05$). Non-survivors did not increase MPV on day 3, $p < 0.05$ but showed 1.3–2.8-fold increases from baseline at time of moribund sacrifice.

Coagulation kinetics: prothrombin time, activated partial thromboplastin time, fibrinogen, and D-dimers

No observable changes were noted in PT or APTT amongst survivors or non-survivors in all dose groups (Supplementary Figure S1). There were significant increases in fibrinogen, which functions in the coagulation cascade as well as an acute phase reactant, in the 7 Gy group on days 8 and 12. In the higher radiation doses of 8 and 10 Gy, when compared to baseline, increases were noted earlier on day 3 ($p < 0.001$), with persistence later to days 15 ($p < 0.001$) and 17 ($p = 0.005$) for the 8 Gy group. Evidence of fibrinolytic activity post radiation was modest with 10% increases of D-dimer on day 3 for all dose groups when compared to baseline values.

Hematologic findings at time of death

Of the decedents in study 2, 9/14 (65%) demonstrated greater than 30% drop in hematocrit at time of death (Table 10). Similarly, 9/14 demonstrated grade 4 neutropenia. All except one animal had grade 4 lymphopenia. The findings of both severe hemorrhage shock (30% or higher blood loss) and grade 4 neutropenia occurred in 50% of the decedents. Of the 8 decedents demonstrating fever >104, 7 (50%) also demonstrated grade 4 neutropenia.

Serum chemistry findings at time of death

Serum chemistries were obtained at baseline and on days 1, 12, and 30 or time of moribund sacrifice. There were no statistical differences between all dose groups and the control. However, categorical biochemical abnormalities were demonstrated at necropsy, relating to hepatic function, renal function, triglyceride elevation, or hypocalcemia (Table 11). The most frequent abnormality observed at scheduled necropsy on day 30 or at moribund euthanasia was an elevation in the liver enzyme AST. When comparing the elevation of liver transaminases, AST appeared to demonstrate a greater range of values with some animals exceeding 100% of baseline values; ALT fluctuated less. AST increases from baseline were observed in 89.2% (25/28) of all animals studied. Survivors showed fewer abnormalities in biochemistries. Regarding the decedent animals, as demonstrated in Table 11, >100% increases from baseline in BUN, creatinine, AST, bilirubin and triglycerides, were only observed in non-survivors. In moribund sacrificed animals, elevations in serum triglyceride levels were next most frequently observed at 85.7% (12/14). All animals with large elevations in creatinine at necropsy had concomitant increases in BUN. At necropsy five animals, two from 8 Gy and three from the 10 Gy demonstrated elevations in serum biochemistries impacting both liver and kidney function.

Given the abnormalities in hepatic and renal function tests, we investigated whether serum albumin and total protein were impacted since both hepatic dysfunction can lead to decreased albumin and protein synthesis and renal dysfunction can contribute to increased albumin and protein loss in the urine. Most non-survivors (85.7%) demonstrated decreases in both serum albumin and total protein at time of death. Low serum albumin and protein tracked with increases in BUN. Serum calcium decreases were observed at the time of death, which may have been related to the modest decreases in serum albumin, which binds calcium.

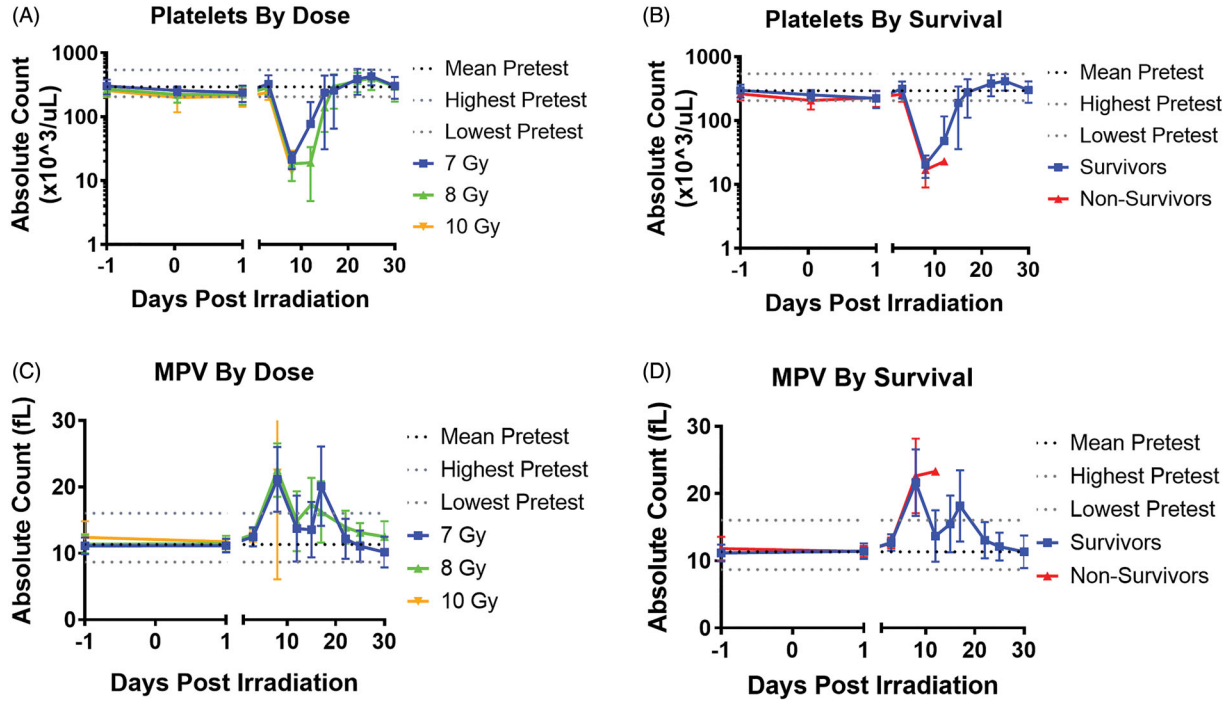

Figure 5. Platelet lineages parameters including platelet count, (A,B), mean platelet volume, MPV (C,D), are shown by dose (A,C) and survivor status (B,D), with mean ± standard deviation per time point respectively. A gap is introduced between days 1 and 2 to represent two separate time scales post- and pre- gap. Horizontal axis days post-irradiation value "−1" indicates a pre-radiation timepoint value and "0" represents the 1-h time point value.

Discussion

The primary objective of this study was to characterize the natural history of acute radiation injury in the NZW rabbit model treated with supportive care. Supportive care components of antibiotics and supplemental hydration were selected based on efficacy observed with these components in our nonhuman primate model of population based care (Yu et al. 2015). With supportive care, we observed 100% lethality at 9 Gy or higher. We also observed the lethality slightly shifted to the right in study 2 with the addition of intravenous hydration.

In humans, the ANC nadir observed following the LD50-100 doses was ≤ 0.5 ($\times 10^9$/L) and was observed 6–9 days following radiation (Mettler et al. 2007). In this NZW model, ANC depletion occurred between 5.4 ± 2.5 and 11.0 ± 4.2 days, with a nadir range of 0.03 ± 0.02–0.18 ± 0.09 ($\times 10^9$/L). The time course and depth of depletion appears to be comparable to human responses suggesting the rabbit model provides meaningful correlation to human conditions. Kinetics of ANC also appeared to follow a pattern previously described clinically (Guskova et al. 1988; Baranov et al. 1989; Mettler et al. 2007). A 10-fold depletion at one hour post-radiation was followed by a rebound at 24 h ranging from 5- to 26-fold increased levels. These findings appeared to be dose dependent. Non-survivors demonstrated the highest rebound granulocytosis on day 1, $>5.2 \times 10^3/\mu$L, and the greatest depletion on day 3, $< 0.1 \times 10^3/\mu$L; such large swings in cell counts observed in the first 3 days post-radiation, identify a critical time period of large pathophysiologic changes warranting additional study. Pinpointing the first 72 h post-radiation as a time interval of significant interest and predictive value has recently been reported using human data analytics, in which blood count data demonstrated >78% positive predictive value (PPV) on day 1 and >90% PPV on day 3 for the development of severe acute radiation syndrome (Port et al. 2017). These findings suggest that the dramatic changes in ANC observed in the first 72 h may be used to predict mortality

In review of human data from irradiated individuals, platelet depletion at LD50–100 exposures of 15–25 ($\times 10^9$/L) was first observed within 7 days post-radiation (Mettler 2007). In our studies, platelet counts of 25.4 ± 45.9–29.4 ± 42.9 ($\times 10^9$/L) were first observed 6–9 days post-radiation. In non-survivors, we observed depletion of platelet counts by 33–60% at 1-h after radiation. It has been reported that within 24 h following radiation, endothelium demonstrates up-regulation of genes coordinating pro-apoptotic and inflammatory pathways; importantly, these pathways are known to regulate the expression of tissue factor, which augments the procoagulant surface of the endothelium (Goldin-Lang, Niebergall, et al. 2007, Goldin-Lang, Pels, et al. 2007). Tissue factor, the transmembrane receptor for Factor VII/VIIa, when bound to the Factor VIIa as a complex, is the key initiator of the extrinsic pathway, activating Factors IX and X for the formation of thrombin(Mackman 2009). The sequential steps of platelet adhesion, activation and aggregation are dependent on platelet binding to endothelial von Willebrand factor but the process is reinforced by locally produced thrombin(Nieswandt et al. 2011). These findings suggest that endothelial injury following radiation may account for the 33–60% drop observed in platelet counts 1 h after radiation exposure, either decreasing the number of circulating cells secondary to increased adhesiveness or perhaps through increased extravasation due to changes in endothelial permeability.

Table 10. Conditions contributing to mortality (study 2).

Dose (Gy)	Days of survival	Euthanasia criteria	Fever	Neutropenia	Lymphopenia	HCT drop	Brain	Lung	Heart	Liver	Intestine	Kidney
7	1	2,3,5	None	None	Grade 4A	7.40%	Seizure like activity	Hemorrhage		Hemorrhage		Tubular injury
8	1	1,2,3,5	None	None	Grade 4A	18.40%	Seizure like activity			Necrosis		
10	5	2	105.8	Grade 4	Grade 4	52%		Thrombi			Hemorrhage	Tubular injury
10	5	2,3,5	104.2	Grade 4	Grade 4B	17.70%	Head tilt	Bacterial colonies		Bacterial colonies		Bacterial colonies
10	7	6	None	Grade 4	Grade 4B	60%			Cardiac petechiae			Tubular injury
10	9	2,3,5	105.8	Grade4	Grade 4	97%	Seizure like activity			Bacterial colonies		Glomerular damage
10	9	1,2,3	100.6	Grade4	Grade 4	63.40%		Bacterial colonies		Bacterial colonies	Hemorrhage	
8	10	1,2,3	None	Grade 3	Grade 4A	38.50%		Hemorrhage		Necrosis	Hemorrhage	
8	11	1,2,3,5	104.7	Grade 4	Grade 4	14.60%		Bacterial colonies				Bacterial colonies
8	11	Found dead	106.6	Grade 3	Grade 4A	17.80%		Bacterial colonies		Bacterial colonies		Bacterial colonies
7	12	5	105.6	Grade 4	Grade 3	52.70%	Head tilt		Hemorrhage		Hemorrhage	
8	12	2,3	none	Grade 3	Grade 4A	35.50%		Hemorrhage				
8	12	2,3	106.1	Grade 4	Grade 4A	39.60%				Bacterial colonies		Bacterial colonies
8	13	1	105.7	Grade 4	Grade 4B	50.30%	Head tilt	Hemorrhage, bacteria				Tubular injury

The magnitude of platelet count drop at 1-h may reflect the extent of endothelial injury and may be used to predict mortality.

Increases in platelet volume were observed at 24 h in non-survivors and at 30 days in survivors. Increases in mean platelet volume indicates larger, more reactive platelets resulting from increased platelet turnover(Martin et al. 1983) and serves as a measure of the functional status of platelet activation (Slavka et al. 2011; Ntolios et al. 2016). Mean platelet volumes have been associated with increased cardiovascular risk (Chu et al. 2010). The observed increases in mean platelet volumes may serve as a link between early platelet loss, hyperthrombotic platelets and the accelerated cardiovascular risk observed in humans following radiation.

We observed increased numbers of immature red blood cells at 1-h post-radiation injury along with increased HCT; this acute increase suggests the bone marrow is responding to radiation by releasing immature red blood cells into circulation, as supported by the observed increases in MCV. The observation that non-survivors failed to sustain a bone marrow response showing large decreases in reticulocyte counts, suggests a differential capacity of the bone marrow to respond between the 7 and 8 Gy doses and the more destructive 10 Gy. Reticulocyte counts may serve as a biomarker to measure the magnitude of bone marrow injury. Additional studies of the bone marrow compartment may be required to confirm the significance of this finding.

We observed early depletion of monocytes in non-survivors. These findings may be relevant to radiation-induced endothelial injury because critical numbers of monocytes play an important role in maintaining endothelial integrity (Quintar et al. 2017) through the inhibition of endothelial apoptosis (Auffray et al. 2007; Hanna et al. 2011; Carlin et al. 2013; McArdle et al. 2015). In an additional mechanism, monocytes when encountering sub-fluent endothelial cells, are triggered to produce endothelial growth factor, angiopoietin-1 and this encounter also leads to endothelial production of Tie-2 (Schubert et al. 2011). Non-survivors showed early depletion of monocytes on day 3 suggesting a potential lack of protective and pro-regenerative monocytes which may adversely affect endothelial repair and regeneration associated with survival. Since animals that had a monocyte count above 0.03×10^3 cells/μL on day 3 significantly ($p < 0.001$) outlived animals that had AMC below that cutoff, early monocyte depletion may serve as a biomarker of the magnitude of endothelial injury.

Five of fourteen non-survivors manifested with signs of inflammatory response syndrome which included more than one of the following criteria: fever, neutropenia, thrombocytopenia, tachycardia, tachypnea, and altered mental status without the identification of bacteria in tissues sampled. These criteria fit the condition of sterile inflammation, a noninfectious process associated with acute tissue injury and innate immune activation (Vincent et al. 2013). Increased pattern recognition receptors, i.e. Toll-like receptors (TLR) and the nucleotide-binding oligomerization domain (NOD) protein families along with up-regulated pathways of leukocyte extravasation and FC receptor phagocytosis, and

Table 11. Biochemical Parameters of Irradiated Rabbits at Necropsy (Study 2).

Dose (Gy)	Days of Survival	Calcium	Chloride	Glucose	Potassium	Sodium	BUN	Creatinine	Albumin	AST	ALT	Total Bilirubin	Total Protein	Triglyceride	Overall score
Normative range		13.48 ± 0.44 (mg/dL)	102.94 ± 3.4 (mm/L)	135.09 ± 10.66 (mg/dL)	4.25 ± 0.31 (mE/L)	141.69 ± 3.35 (mM/L)	14.16 ± 2.24 (mg/dL)	1.14 ± 0.15 (mg/dL)	3.88 ± 0.25 (g/dL)	13.41 ± 5.40 (U/L)	23.33 ± 7.33 (U/L)	0.13 ± 0.02 (U/L)	5.14 ± 0.31 (g/L)	69.88 ± 31.55 (mg/dL)	
7	1	1	0	0	3	0	3	3	0	NA	NA	3	0	3	16
8	1	1	1	1	2	0	3	3	1	3	NA	2	1	3	21
10	5	1	0	0	0	0	3	2	1	3	2	1	1	2	16
10	5	1	0	2	0	0	3	1	1	1	1	0	1	3	14
10	7	1	0	1	0	0	3	0	1	2	1	1	1	1	12
10	9	2	0	2	3	0	3	3	1	3	1	1	1	2	22
10	9	0	0	1	3	0	3	3	1	3	NA	1	1	3	19
8	10	1	0	1	0	0	2	1	1	2	2	1	1	2	14
8	11	1	0	0	1	0	3	0	1	3	NA	1	1	1	12
8	11	1	0	2	2	0	1	2	1	3	3	3	1	1	20
8	12	1	0	0	0	0	0	0	1	1	1	1	1	0	6
8	12	0	0	0	1	0	1	0	1	1	1	0	0	3	8
7	12	1	0	0	0	0	1	0	1	1	1	1	1	3	10
8	13	1	0	0	1	0	1	1	0	1	1	1	0	1	8
8	30	0	0	1	0	0	0	1	0	0	1	0	0	0	3
8	30	0	0	1	0	0	0	1	0	1	1	0	0	0	4
8	30	0	0	1	0	0	1	1	0	1	0	1	0	0	5
8	30	0	0	0	0	0	1	0	0	1	1	0	0	1	4
7	30	0	0	1	1	0	1	0	0	2	1	0	0	1	7
7	30	0	0	0	1	0	1	1	0	1	NA	0	0	1	5
7	30	0	0	1	0	0	0	0	0	0	0	1	0	1	3
8	30	0	0	1	0	0	1	1	0	1	0	1	0	1	6
7	30	0	0	0	0	0	0	0	0	1	1	1	0	1	4
7	30	0	0	1	0	0	0	0	0	0	2	0	0	2	5
7	30	0	0	1	0	0	1	1	0	1	0	1	0	2	7
8	30	0	0	1	1	0	0	0	0	1	1	1	0	2	7
7	30	0	0	1	1	0	1	1	1	1	1	0	1	2	10
8	30	0	0	1	0	0	0	1	0	1	0	0	0	3	6

Notes. 0= [normal range] ± 10% ; 1 = ± >10%–50% & outside the normal range; 2 = ± >50%–100% & outside the normal range; 3 = ± >100% &outside the normal range, NA: not available. * value analyzed was the last available value

signaling by IL-6, IL-10, TREM1, ephrin receptor, actin cytoskeleton, B cell receptor have characterized this condition (Nathan and Ding 2010; Xiao et al. 2011). These measures may have utility in further characterization of the natural history of radiation in this model and may also be potential targets for mitigation.

Last, we observed markers of organ dysfunction on day 1 to track with mortality. Elevations in BUN tracked with renal pathology at time of moribund sacrifice with more than a 4-fold increased likelihood of mortality if the day 1 post-radiation BUN level exceeded 56 mg/dL. Findings of decreased albumin tracked with increases in BUN suggesting decreased albumin was likely due to renal dysfunction and urinary loss. Such findings have been previously described in the irradiated rat model; marked changes in the urinary proteome consequent to radiation-induced renal injury were described as early as 24 h post-radiation and are being studied as prognostic indicators (Sharma et al. 2008). AST also appeared to track with mortality. We observed liver histopathology in the rabbit tissues of animals with elevations in ALT and AST, suggesting elevation of these serum biochemistries likely reflect liver injury. AST elevation on day 1 was associated with mortality and appears to provide a sensitive indicator for radiation induced, acute liver injury. Notably, increased serum lipid levels appear to be a difference between the rabbit and human responses to acute radiation.

Conclusions

Animal models of the hematopoietic acute radiation syndrome have been reported using rodents, dogs, rhesus macaques, and recently, the Gottingen minipig. The NZW rabbit is technically feasible to study as it allows monitoring of relevant clinical parameters, and effective blood sampling. Hematopoietic depletion kinetics and predictors of mortality in NZW rabbits are highly congruent to those described in human victims of radiation injury (Guskova et al. 1988; Baranov et al. 1989; Mettler et al. 2007). Under the FDA Animal Rule guidance, where standard clinical trials are not possible due to the nature of the exposure to lethal or permanently disabling agents (i.e. chemical, biological, radiological, or nuclear substances), the NZW rabbit model of ARS is an attractive model for further development and testing of medical countermeasures.

Acknowledgments

Funding for this project has been provided in whole or in part by the Biomedical Advanced Research and Development Authority, Office of the Assistant Secretary for Preparedness and Response, Office of the Secretary, Department of Health and Human Services, under contract no. HHS0100201500008I.

Authors contributions

Paredes, Lindeblad, and Bartholomew wrote the paper. Lindeblad, Bartholomew, Moulder, Nanda, and Lyubimov designed the study. Paredes, Patil, Hong, Smith, Mousefeiris, and Bosland conducted data acquisition. Paredes, Patil, Neal, Nanda, Mousafeiris, Bosland, Lyubimov, and Bartholomew analyzed the data.

Disclosure statement

The authors have no conflicts of interest to report.

Notes on contributors

Andre Paredes, PhD, is a Research Assistant Professor in the Department of Surgery at the University of Illinois at Chicago. He received is PhD in Bioengineering in 2018. His research interest are in photomedicine, innate immunity, and radiation biology.

Mr. Matthew Lindeblad is the Director of the Toxicology Research Laboratory (TRL) at the University of Illinois at Chicago over. He served as a Co-PI or Study Director on contracts for more than 22 years, including BARDA (radiation studies in mice, rabbits, mini-pigs and monkeys), NIAID, NCI, DOD, and CDC.

Rachana Patil, MS, is a Research Scientist at Pediatrics Stem Cell Transplant Division at Stanford University. She has 8 years of experience in technical project leadership, laboratory management, and other academic services. Her research improves outcomes of allogeneic hematopoietic stem cell transplant in children with various leukemia and genetic disorders.

Matthew D. Neal, MD FACS is the Roberta G. Simmons Associate Professor of Surgery at the University of Pittsburgh. He is the Director of the Pittsburgh Trauma Research Center and is a practicing trauma surgeon. His research focuses on mechanisms of hemostasis, coagulopathy, and thrombosis, funded by NIH and DoD.

Yuanfan Hong is a Research Scientist at the Transplantation Biology Research Laboratory at the University of Illinois. She has over 10 years of experience in cellular and molecular assays, laboratory management and data analytics. Her research focuses on radiation biology and cellular therapeutics.

Brett Smith is a Licensed Radiophysicist at the University of Illinois with a clinical interest in radiation therapeutics. Additional interests include large and small animal models of radiation exposure.

Joy P. Nanda, DSc, MS, MHS, MBA, is a Community, Behavioral, and Statistical Epidemiologist from Johns Hopkins with over four decades of experience in teaching, research, mentoring, and other academic/community services/consultations on epidemiological and biostatistical methodologies. Joy currently devotes his time in COVID-19 recovery evaluation and community engaged translational research.

Vasileios Mousafeiris is an MD and Surgery Resident. He received his MSc in Medicinal chemistry and Pathology in 2018. His main research interests include tissue regeneration, radiology and cancer profile.

John Moulder, PhD is Professor Emeritus of Radiation Oncology at the Medical College of Wisconsin. His primary research interest is the development of methods to detect, prevent and treat injuries from radiation exposure. A secondary interest is explaining radiation exposure risks to those who are not radiation experts.

Maarten C. Bosland, DVSc, PhD, is a Professor in the Department of Pathology at the University of Illinois at Chicago. He is a laboratory animal pathologist providing pathology services to investigators. His research interests include hormonal carcinogenesis, prostate cancer, cancer chemoprevention, and experimental pathology conducting NIH and DoD-funded projects.

Alexander Lyubimov, MD, PhD, DABT, is a Research Associate Professor, Department of Pharmacology at UIC. He has received his PhD in Toxicology in 1989. His interests are drug development, efficacy and toxicity of the new drugs for many different indications,

including cancer, acute radiation syndrome, diabetes, thrombosis, sepsis, etc.

Amelia Bartholomew is Chief of Translational Research and Professor of Surgery and Bioengineering at the University of Illinois Chicago. She is interested in hematopoietic, coagulopathic and inflammatory responses following total body radiation. Additional interests include cellular therapeutics in tissue regeneration and cancer treatments.

ORCID

Andre Paredes http://orcid.org/0000-0001-6949-9549
John Moulder http://orcid.org/0000-0002-6217-9611

References

AFRRI, and Armed Forces Radiobiology Research Institute. 2003. Medical management of radiobiological casualties – handbook. P. 1–147.

Andrews HL. 1958. Species differences in response to high radiation doses. Radiat Res. 9(4):469–477.

Anno GH, Baum SJ, Withers HR, Young RW. 1989. Symptomatology of acute radiation effects in humans after exposure to doses of 0.5–30 Gy. Health Phys. 56(6):821–838.

Auffray C, Fogg D, Garfa M, Elain G, Join-Lambert O, Kayal S, Sarnacki S, Cumano A, Lauvau G, Geissmann F. 2007. Monitoring of blood vessels and tissues by a population of monocytes with patrolling behavior. Science. 317(5838):666–670.

Baranov A, Gale RP, Guskova A, Piatkin E, Selidovkin G, Muravyova L, Champlin RE, Danilova N, Yevseeva L, Petrosyan L. 1989. Bone marrow transplantation after the Chernobyl nuclear accident. N Engl J Med. 321(4):205–212.

Bolus NE. 2001. Basic review of radiation biology and terminology. J Nucl Med Technol. 29(2):67–73.

Broerse JJ, Macvittie T. 2012. Response of different species to total body irradiation. New York: Springer Science and Business Media.

Broerse JJ, Van Bekkum DW, Hollander CF, Davids JA. 1978. Mortality of monkeys after exposure to fission neutrons and the effect of autologous bone marrow transplantation. Int J Radiat Biol Relat Stud Phys Chem Med. 34(3):253–264.

Carlin LM, Stamatiades EG, Auffray C, Hanna RN, Glover L, Vizcay-Barrena G, Hedrick CC, Cook HT, Diebold S, Geissmann F. 2013. Nr4a1-dependent Ly6C(low) monocytes monitor endothelial cells and orchestrate their disposal. Cell. 153(2):362–375.

Carsten AL. 1984. Acute lethality—the hemopoietic syndrome in different species. In: Response of different species to total body irradiation. New York: Springer Science & Business Media; 59–87.

Chu SG, Becker RC, Berger PB, Bhatt DL, Eikelboom JW, Konkle B, Mohler ER, Reilly MP, Berger JS. 2010. Mean platelet volume as a predictor of cardiovascular risk: a systematic review and meta-analysis. J Thromb Haemost. 8(1):148–156.

Dainiak N. 2018. Medical management of acute radiation syndrome and associated infections in a high-casualty incident. J Radiat Res. 59(Suppl_2):ii54–ii64.

Eldred E, Trowbridge WV. 1954. Radiation sickness in the monkey. Radiology. 62(1):65–73.

Fan J, Kitajima S, Watanabe T, Xu J, Zhang J, Liu E, Chen YE. 2015. Rabbit models for the study of human atherosclerosis: from pathophysiological mechanisms to translational medicine. Pharmacol Ther. 146:104–119.

FDA. 2009. Guidance for industry: animal models, essential elements to address efficacy under the animal rule. Rockville, MD: Division of Dockets Management (HFA-305), US Food and Drug Administration. p. 1–19.

Gitel SN, Wessler S. 1983. Dose-dependent antithrombotic effect of warfarin in rabbits. Blood. 61(3):435–438.

Goldin-Lang P, Niebergall F, Antoniak S, Szotowski B, Rosenthal P, Pels K, Schultheiss HP, Rauch U. 2007. Ionizing radiation induces upregulation of cellular procoagulability and tissue factor expression in human peripheral blood mononuclear cells. Thromb Res. 120(6):857–864.

Goldin-Lang P, Pels K, Tran QV, Szotowski B, Wittchen F, Antoniak S, Willich T, Witt H, Hummel M, Lenze D, et al. 2007. Effect of ionizing radiation on cellular procoagulability and co-ordinated gene alterations. Haematologica. 92(8):1091–1098.

Grahn D, Sacher GA, Walton H. Jr. 1956. Comparative effectiveness of several x-ray qualities for acute lethality in mice and rabbits. Radiat Res. 4(3):228–242.

Guskova AK, Barabanova AV, Baranov A, Gruszdev G, Pyatkin Y, Nadezhina NM, Metlyaeva NA, Selidovkin GD, Moiseev AA, Gusev IA, et al. 1988. Appendix: Acute radiation effects in victims of the Chernobyl nuclear power plant accident. p. 613–647.

Hanna RN, Carlin LM, Hubbeling HG, Nackiewicz D, Green AM, Punt JA, Geissmann F, Hedrick CC. 2011. The transcription factor NR4A1 (Nur77) controls bone marrow differentiation and the survival of Ly6C-monocytes. Nat Immunol. 12(8):778–785.

Henschke UK, Morton JL. 1957. Mortality of rhesus monkeys after single total body irradiation. Am J Roentgenol Radium Ther Nucl Med. 77(5):899–909.

Hewitt CD, Innes DJ, Savory J, Wills MR. 1989. Normal biochemical and hematological values in New Zealand white rabbits. Clin Chem. 35(8):1777–1779.

IAEA. 1998. Diagnosis and treatment of radiation injuries. Safety series. Vienna: International Atomic Energy Agency.

Jimoh OA, Ewuola EO. 2018. Thermophysiological traits in four exotic breeds of rabbit at least temperature-humidity index in humid tropics. JoBAZ. 79(1):18.

Jones TD, Morris MD, Wells SM, Young RW. 1986. Animal mortality resulting from uniform exposures to photon radiations: calculated LD50s and a compilation of experimental data. Oak Ridge, TN: Oak Ridge National Lab.

Mackman N. 2009. The role of tissue factor and factor VIIa in hemostasis. Anesth Analg. 108(5):1447–1452.

MacVittie TJ, Farese AM, Jackson W. 3rd. 2005. Defining the full therapeutic potential of recombinant growth factors in the post radiation-accident environment: the effect of supportive care plus administration of G-CSF. Health Phys. 89(5):546–555.

Mapara M, Thomas BS, Bhat KM. 2012. Rabbit as an animal model for experimental research. Dent Res J (Isfahan.). 9:111–118.

Martin JF, Trowbridge EA, Salmon G, Plumb J. 1983. The biological significance of platelet volume: its relationship to bleeding time, platelet thromboxane B2 production and megakaryocyte nuclear DNA concentration. Thromb Res. 32(5):443–460.

McArdle S, Chodaczek G, Ray N, Ley K. 2015. Intravital live cell triggered imaging system reveals monocyte patrolling and macrophage migration in atherosclerotic arteries. J Biomed Opt. 20(2):26005

Mettler FA, Jr., Gus'kova AK, Gusev I. 2007. Health effects in those with acute radiation sickness from the Chernobyl accident. Health Phys. 93(5):462–469.

Moroni M, Coolbaugh TV, Lombardini E, Mitchell JM, Moccia KD, Shelton LJ, Nagy V, Whitnall MH. 2011. Hematopoietic radiation syndrome in the Gottingen minipig. Radiat Res. 176(1):89–101.

Morris MD, Jones TD. 1989. Hematopoietic death of unprotected man from photon irradiations: statistical modeling from animal experiments. Int J Radiat Biol. 55(3):445–461.

Mouthon MA, Vereycken-Holler V, Van der Meeren A, Gaugler MH. 2003. Irradiation increases the interactions of platelets with the endothelium in vivo: analysis by intravital microscopy. Radiat Res. 160(5):593–599.

Nathan C, Ding A. 2010. Nonresolving inflammation. Cell. 140(6):871–882.

Nieswandt B, Pleines I, Bender M. 2011. Platelet adhesion and activation mechanisms in arterial thrombosis and ischaemic stroke. J Thromb Haemost. 9 (Suppl 1):92–104.

Norris WP, Fritz TE, Rehfeld CE, Poole CM. 1968. The response of the beagle dog to cobalt-60 gamma radiation: determination of the LD50(30) and description of associated changes. Radiat Res. 35(3):681–708.

Ntolios P, Papanas N, Nena E, Boglou P, Koulelidis A, Tzouvelekis A, Xanthoudaki M, Tsigalou C, Froudarakis ME, Bouros D, et al. 2016. Mean platelet volume as a surrogate marker for platelet activation in patients with idiopathic pulmonary fibrosis. Clin Appl Thromb Hemost. 22(4):346–350.

Ozasa K, Takahashi I, Grant EJ. 2016. Radiation-related risks of non-cancer outcomes in the atomic bomb survivors. Ann Icrp. 45(1 Suppl):253–261.

Painter EE, Brues AM. 1949. The radiation syndrome. N Engl J Med. 240(22):871–876.

Paris F, Fuks Z, Kang A, Capodieci P, Juan G, Ehleiter D, Haimovitz-Friedman A, Cordon-Cardo C, Kolesnick R. 2001. Endothelial apoptosis as the primary lesion initiating intestinal radiation damage in mice. Science. 293(5528):293–297.

Peng X, Knouse JA, Hernon KM. 2015. Rabbit models for studying human infectious diseases. Comp Med. 65(6):499–507.

Port M, Pieper B, Knie T, Dorr H, Ganser A, Graessle D, Meineke V, Abend M. 2017. Rapid prediction of hematologic acute radiation syndrome in radiation injury patients using peripheral blood cell counts. Radiat Res. 188(2):156–168.

Quintar A, McArdle S, Wolf D, Marki A, Ehinger E, Vassallo M, Miller J, Mikulski Z, Ley K, Buscher K. 2017. Endothelial protective monocyte patrolling in large arteries intensified by western diet and atherosclerosis. Circ Res. 120(11):1789–1799.

Rust JH, Trum BF, Wilding JL, Simons CS, Comar CL. 1954. Lethal dose studies with burros and swine exposed to whole body cobalt-60 irradiation. Radiology. 62(4):569–574.

Schollnberger H, Eidemuller M, Cullings HM, Simonetto C, Neff F, Kaiser JC. 2018. Dose-responses for mortality from cerebrovascular and heart diseases in atomic bomb survivors: 1950-2003. Radiat Environ Biophys. 57:17–29.

Schubert SY, Benarroch A, Monter-Solans J, Edelman ER. 2011. Primary monocytes regulate endothelial cell survival through secretion of angiopoietin-1 and activation of endothelial Tie2. Arterioscler Thromb Vasc Biol. 31(4):870–875.

Sharma M, Halligan BD, Wakim BT, Savin VJ, Cohen EP, Moulder JE. 2008. The urine proteome as a biomarker of radiation injury: submitted to proteomics- clinical applications special issue: "renal and urinary proteomics (Thongboonkerd)". Proteomics Clin Appl. 2(7–8):1065–1086.

Shirota T, Tavassoli M. 1992. Alterations of bone marrow sinus endothelium induced by ionizing irradiation: implications in the homing of intravenously transplanted marrow cells. Blood Cells. 18(2): 197–214.

Singh VK, Olabisi AO. 2017. Nonhuman primates as models for the discovery and development of radiation countermeasures. Expert Opin Drug Discov. 12(7):695–709.

Singh VK, Newman VL, Berg AN, MacVittie TJ. 2015. Animal models for acute radiation syndrome drug discovery. Expert Opin Drug Discov. 10(5):497–517.

Slavka G, Perkmann T, Haslacher H, Greisenegger S, Marsik C, Wagner OF, Endler G. 2011. Mean platelet volume may represent a predictive parameter for overall vascular mortality and ischemic heart disease. Arterioscler Thromb Vasc Biol. 31(5):1215–1218.

Stenke L, Lindberg K, Lagergren Lindberg M, Lewensohn R, Valentin J, Powles R, Dainiak N. 2018. Coordination of management of the acute radiation syndrome. Radiat Prot Dosimetry. 182(1):80–84.

Suckow MA, Stevens KA, Wilson RP. 2012. The laboratory rabbit. Guinea pig, hamster, and other rodents. New York: Elsevier Academic Press.

Takahashi I, Ohishi W, Mettler FA, Jr.,Ozasa K, Jacob P, Ban N, Lipshultz SE, Stewart FA, Nabika T, Niwa Y, et al. 2013. A report from the 2013 international workshop: radiation and cardiovascular disease, Hiroshima, Japan. J Radiol Prot. 33(4):869–880.

Takatsuka H, Wakae T, Mori A, Okada M, Okamoto T, Kakishita E. 2002. Effects of total body irradiation on the vascular endothelium. Clin Transplant. 16(5):374–377.

Tullis JL, Tessmer CF, Cronkite EP, Chambers FW. 1949. The lethal dose of total-body X-ray irradiation in swine. Radiology. 52(3): 396–400.

Vincent JL, Opal SM, Marshall JC, Tracey KJ. 2013. Sepsis definitions: time for change. Lancet. 381(9868):774–775.

Wang Y, Boerma M, Zhou D. 2016. Ionizing radiation-induced endothelial cell senescence and cardiovascular diseases. Radiat Res. 186(2):153–161.

Waselenko JK, MacVitte TJ, Blakely WF. 2004. Medical management of the acute radiation syndrome: recommendations of the strategic national stockpile radiation working group. Ann Intern Med. 140(12):1037–1051.

Williams JP, Brown SL, Georges GE, Hauer-Jensen M, Hill RP, Huser AK, Kirsch DG, Macvittie TJ, Mason KA, Medhora MM, et al. 2010. Animal models for medical countermeasures to radiation exposure. Radiat Res. 173(4):557–578.

Xiao W, Mindrinos MN, Seok J, Cuschieri J, Cuenca AG, Gao H, Hayden DL, Hennessy L, Moore EE, Minei JP, et al.; Inflammation, and Program Host Response to Injury Large-Scale Collaborative Research. 2011. A genomic storm in critically injured humans. J Exp Med. 208(13):2581–2590.

Yu JZ, Lindeblad M, Lyubimov A, Neri F, Smith B, Szilagyi E, Halliday L, MacVittie T, Nanda J, Bartholomew A. 2015. Subject-based versus population-based care after radiation exposure. Radiat Res. 184(1): 46–55.

Zoetelief J, Wagemaker G, Broerse JJ. 1998. Dosimetry for total body irradiation of rhesus monkeys with 300 kV X-rays. Int J Radiat Biol. 74(2):265–272.